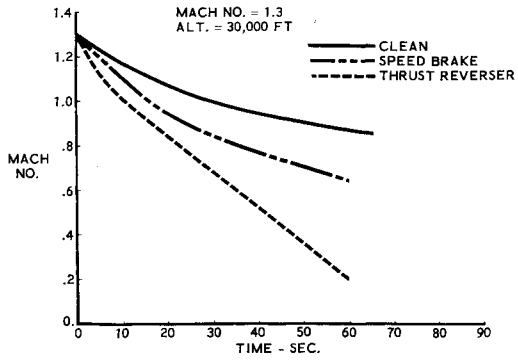

FIGURE 8 DECELERATION AT 30,000 FEET FROM M = 1.3

Fig. 8 Deceleration at 30,000 ft from $M = 1.3$.

out the region and was rated operationally acceptable by the pilots. The airplane was also decelerated from Mach 1.3 to 0.9 by reducing the throttle to the idle setting without deflection of a drag device. The airplane behaved in the same manner quantitatively and qualitatively as with application of the thrust reverser. However, time to decelerate was longer and there was no initial pitchup with reduction of throttle. Speed instability existed throughout the transonic area.

In Fig. 8, deceleration times are presented for an initial Mach number of 1.3 at 30,000 ft in the same manner as for the subsonic decelerations. Again, the thrust-reverser mechanization provided performance and handling qualities superior to those of the speed-brake equipped airplane.

Summary

The thrust-reverser equipped airplane was preferred over the clean or speed-brake configurations for deceleration because of the increased retardation available from the thrust reverser without adverse effects on the handling qualities.

Conclusions

1) In general, a thrust reverser could improve the over-all mission effectiveness.

2) In gross decelerations of both subsonic and supersonic speeds, an airplane equipped with a thrust reverser can provide performance handling qualities superior to an airplane equipped with speed brakes.

3) For an instrument approach under ILS conditions, the advantages of the thrust reverser in speed control and application of power at wave-off did not seem sufficient to balance the disadvantages of unconventional cockpit controls and possible pitching moments resulting from application of the reverser.

4) An integrated thrust-reverser/throttle controller was the most desired thrust-reverser control mechanism for all flight modes with the exception of the ILS approaches, where it was not employed.

References

[1] Anderson, S. B. et al, "Flight Measurements of the Effect of a Controllable Thrust Reverser on the Flight Characteristics of a Single-Engine Jet Airplane," Memo 4-26-59A, 1959, NASA.

[2] O'Hara, F., "Handling Criteria," *Journal of the Royal Aeronautical Society*, April 1967.

MAY-JUNE 1969 J. AIRCRAFT VOL. 6, NO. 3

Opening Time of Parachutes Under Infinite-Mass Conditions

H. G. HEINRICH*
University of Minnesota, Minneapolis, Minn.

For the infinite-mass case, defined by the ratio of the suspended to the canopy included masses, equations have been developed which provide the canopy filling time for solid cloth as well as for ribbon and ringslot parachutes. Using newly established experimental data of the rate of canopy growth, the results obtained by this method agree satisfactorily with empirical information given in the *United States Air Force Parachute Handbook*.

Nomenclature

a,b = const
A = $t_f D_0^2/\pi$
B = $(\pi d_v/2D_0)^2$
C = u/v, coefficient of effective porosity
C_p = pressure coefficient
C_D = drag coefficient
C_DS = drag area
d = instantaneous diameter of parachute inlet
d_v = vent hole diameter
D_{max} = maximum diameter of parachute
D_0 = nominal diameter of parachute
D_p = instantaneous maximum projected diameter of parachute
D_{pc} = drag of parachute canopy
D_{ps} = projected diameter under steady-state condition
D_s = drag of suspended weight
$\dot{m}$ = actual mass flow, slugs/sec
m_a = apparent mass
m_i = mass of included air
$\dot{m}_i$ = ideal mass flow, slugs/sec
m_p = mass of parachute
m_s = mass of suspended weight
Δ_p = pressure differential
S_0 = total area of parachute
S_p = instantaneous projected area of parachute
t = time
t_f = filling or inflation time
T = t/t_f, dimensionless filling-time ratio
u = average velocity over the porous or slotted area
V = velocity; included volume of parachute canopy

Presented as Paper 68–12 at the AIAA 6th Aerospace Sciences Meeting, New York, January 22–24, 1968; submitted January 12, 1968; revision received October 2, 1968. This study has, in part, been sponsored by the U.S. Air Force, Contract AF33(615)–5029.

* Professor. Associate Fellow AIAA

V_g = exit velocity through the slots of the canopy
V_{in} = velocity of flow entering the inlet
V_{max} = maximum included volume at end of inflation
V_s = velocity at instant of snatch
V_v = velocity of flow leaving the vent
V_∞ = freestream or system velocity
W_p = weight of parachute canopy
W_s = suspended weight
α_0 = $\bar{V}_v/V_\infty$
η = efficiency or flow coefficient
λ_g = over-all geometric porosity
λ'_g = geometric porosity in the ribbon grids
λ_{gcrit} = critical porosity
ρ = density

Superscript

$\overline{(\ )}$ = averaged quantity

I. Introduction

THE equation of motion of the parachute inflation includes as significant terms the suspended weight, the size of the parachute canopy, the instantaneous velocity, and the canopy enclosed and apparent masses and their time derivatives. A number of methods of mathematical presentation of the calculation of the parachute-opening dynamics have been proposed, and their degree of complexity depends almost entirely on the simplifications and empirical terms which they encompass.

The most analytically oriented opening-process theory, shown in the *Air Force Parachute Handbook*,[1] is based on original work by O'Hara,[2] and can be modified to yield, as closed solution, the opening time of parachutes under infinite-mass condition. However, this has not been attempted so far, probably because of lack of information of the variation of the nonsteady terms and a satisfactory mathematical definition of the infinite-mass condition.

The following study uses the proposed canopy geometry by O'Hara,[2] but introduces a new experimentally determined canopy size-time function and a definition of the infinite-mass case. This method leads to a closed form solution and yields results which agree very well with empirical data of Ref. 1.

II. Canopy Size-Time Function

In the equation of motion, the area and the volume or mass terms are very influential during the parachute inflation,[3] and their satisfactory determination under infinite-mass condition is very important. O'Hara[2] derived them for the finite case from the parachute geometry, but they can also be determined experimentally in drop tests or in a wind tunnel. Both methods are cumbersome, whereas the wind-tunnel method is probably a little easier to accomplish. For wind-tunnel experiments duplicating the infinite-mass case, one has merely to record the inflation process while the suspension point of the parachute is held at a fixed position. For finite-mass tests, this point has to be movable as shown in Ref. 3.

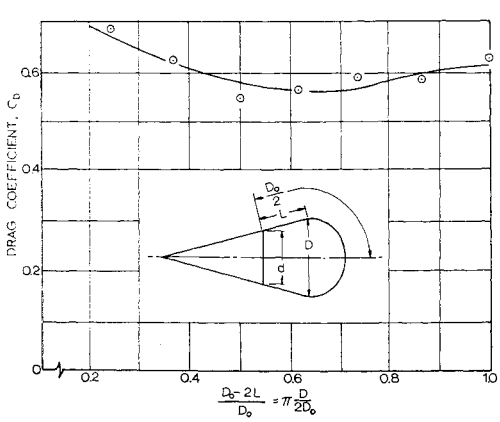

Fig. 1 Drag coefficient of O'Hara shapes under steady-state condition.[11]

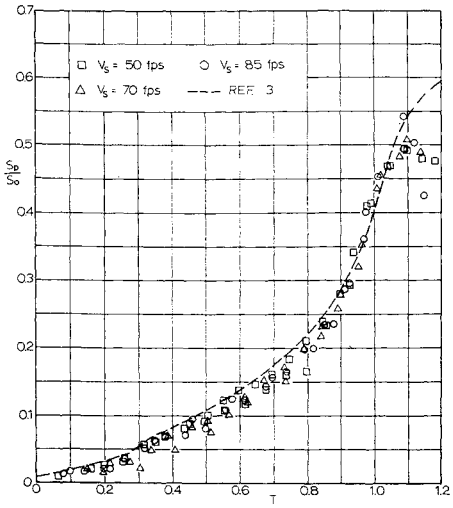

Fig. 2 Ratio of projected and total canopy area vs time; solid, flat parachute, infinite-mass condition.

The Air Force Parachute Handbook[1] utilizes in its opening shock theory a linear drag area-time relationship, which, in connection with a constant drag area vs the diameter ratio, $\pi D_p/2D_0$, Fig. 1, and the geometry by O'Hara,[2] leads to a relatively simple mode of calculation. It is worthwhile to note that this method provides for finite-mass cases acceptable values for the maximum parachute force. Also, Pflanz[4] has shown that the maximum opening force of a parachute load system, which is decelerated merely by the parachute drag, varies insignificantly when the second time derivative of the drag area-time function is zero, positive, or negative. This statement is, of course, valid only within certain limits.

Newer studies of full-size, solid, flat parachutes under finite-mass conditions by Berndt[5] and Berndt and DeWeese[6] have, however, shown that size-time relationships of actual parachutes deviate considerably from a linear course. Also, wind-tunnel tests[3] with solid, flat parachute models indicated more complicated curvatures. Unfortunately, size-time functions of full-size parachutes under infinite-mass conditions are presently not available. Therefore, wind-tunnel studies were made in which solid, flat, and ringslot parachutes inflated under infinite-mass conditions and the front and side profiles were filmed with approximately 2000 frames/sec. From these pictures, the projected area with respect to time was determined and is shown in Figs. 2 and 3.

In Fig. 2, one notices that the area-time relationships under finite- and infinite-mass conditions up to $T = 1$ are practically identical. Therefore, one may use the area-time functions of Ref. 3, namely, $D_p/D_0 = 0.097 + 0.471T$, and $D_p/D_0 = 1.4 - 2.8T + 2.05T^2$ for the regions of $0 < T < 0.8$ and $0.8 \leq T \leq 1.0$, respectively. It is also of certain interest to note that Fig. 2 indicates that a solid, flat parachute in the finite-mass case overinflates much more than under infinite-mass condition.

Figure 3 shows the area-time function of a ringslot or ribbon parachute which for the infinite-mass case and as first approximation, and also in view of Pflanz,[4] will be replaced for the time being by a straight line. With this simplification, the size-time function of a ringslot or ribbon parachute can be presented then as $D_p/D_0 = 2T^{1/2}/\pi$ as derived in Ref. 1.

As a matter of interest, the area-time relationship of the same parachute model, but under finite-mass condition, is illustrated. One notices characteristic differences as before for the solid, flat parachute under infinite- and finite-mass conditions. Both curves are, however, so far merely based on wind-tunnel experiments. The approximation suggested

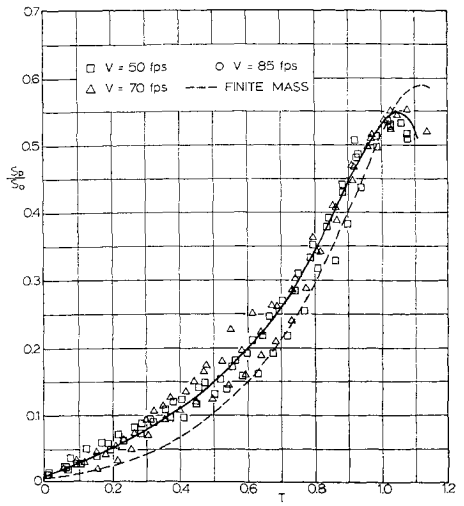

Fig. 3 Ratio of projected and total canopy area vs time; ringslot ribbon parachute, 15% porosity, infinite-mass condition.

previously will first be tried and the results compared with available information of full-size tests.

III. Infinite-Mass Condition

Under infinite-mass condition one understands a process in which the systems velocity during the parachute inflation remains practically constant. Such processes occur often in reality. The inflation, however, follows the equation of motion which can be written[3] as

$$(d/dt)[(m_s + m_p + m_i + m_a)V] = (W_s + W_p)\sin\alpha - D_s - D_{pc} \quad (1)$$

In general and for simplicity, one can set $W_s \gg W_p$, $D_{pc} \gg D_s$, $\alpha = 0$, or $\alpha = \pi/2$. Equation (1), simplified and rearranged, amounts to

$$m_s \frac{dV}{dt} = m_s g - \frac{\rho}{2} C_D S V^2 - V\left(\frac{dm_i}{dt} + \frac{dm_a}{dt}\right) - (m_p + m_i + m_a)\frac{dV}{dt} \quad (2)$$

In this equation one notices two mass terms, namely, the suspended mass m_s and the group in the parenthesis. If the group, compared with the other terms, is very small, the contribution of the last term of Eq. (2) to the total deceleration force is insignificant and may be neglected. This raises the question of how large this group may be in order to satisfy this condition. Under these circumstances, the term infinite mass is then strictly related to the suspended mass m_s, and the probable velocity decay is calculated in the following.

First a ratio of $m_s/(m_p + m_i + m_a) = 100$ has been arbitrarily selected. This ratio represents, for a 4-ft or a 28-ft solid, flat parachute, suspended masses of 1.405 slugs (45 lb) and 540.5 slugs (17,410 lb), respectively.

Furthermore, an approximate filling time and a drag area-time relationship has to be assumed. For this purpose the filling times t_f were determined from the experimental curves of Ref. 1 for infinite-mass cases. These values were combined with canopy size-time functions as proposed in Refs. 1 and 3. In this manner essentially two independent calculations were made. The calculation using the filling-time information and the size-time function of Ref. 1 yielded a velocity change of $\Delta V = 0.01\ V_s$. Performing the same calculation with the size-time function from Ref. 3, the velocity decay amounts to $\Delta V = 0.03\ V_s$.

It can be shown that the velocity decay of a ribbon parachute-load system with similar surface loading is in the same order. In summary, one can say that these velocity changes during the parachute inflation are small enough and that a mass ratio of $m_s/(m_p + m_i + m_a) = 100$ practically represents the condition of an infinite-mass case.

IV. Mass-Balance Equation

Having established the rate of canopy growth, one may apply the continuity equation and determine the mass imbalance which develops the included mass and causes the parachute to inflate. In order to encompass all conventional parachutes, the mass-balance equation will be written for a parachute with geometric or inherent porosity, such as ribbon or ringslot parachutes. Later, the geometric porosity of the ribbon grid[7] will be expressed in terms of effective cloth porosity,[8,9] and in this form the equation can be directly applied to solid cloth parachutes. Since the effective porosity of cloth varies with the air density, this approach incorporates then also the so-called parachute altitude effects.[10]

The rate of change of the included mass equals the difference between the mass fluxes entering the inlet and leaving through the porous area of the canopy. The cloth porosity of the ribbons or the concentric rings of the ringslot parachute will, for the time being, be neglected. The mass balance then can be expressed as

$$\frac{d}{dt}(\rho V) = \rho\frac{\pi}{4} d^2 \bar{V}_{in} - \rho\lambda'_g\pi\left(\frac{D_p^2}{2} - \frac{d_v^2}{4}\right)\bar{V}_g - \rho\pi\frac{d_v^2}{4}\bar{V}_v \quad (3)$$

where λ'_g is the geometric porosity of the canopy excluding the vent. Equation (3) includes the assumption that the outflow through the porous area occurs merely on the hemispherical roof portion, which fact, to a certain extent, has been verified through wind-tunnel experiments.

Considering only the subsonic flow regime and realizing that during the inflation the air density varies insignificantly, one may eliminate the density ρ, divide by the system velocity V_∞, and obtain from Eq. (3)

$$\frac{1}{V_\infty}\frac{dV}{dt} = \frac{1}{V_\infty t_f}\frac{dV}{dT} = \pi\left(\frac{d}{2}\right)^2\frac{\bar{V}_{in}}{V_\infty} - \pi\left(\frac{d_v}{2}\right)^2\frac{\bar{V}_v}{V_\infty} - \lambda'_g\pi\left(\frac{D_p^2}{2} - \frac{d_v^2}{4}\right)\frac{\bar{V}_g}{V_\infty} \quad (4)$$

For a ribbon or ringslot parachute, the ratios representing the flow through the inlet and the vent outflow, $\bar{V}_{in}/V_\infty$ and $\bar{V}_v/V_\infty$, respectively, have been determined by wind-tunnel experiments.[11] Results are shown in Fig. 4. It can be seen that the velocity through the vent varies very little, is almost equal to the freestream velocity, and may be abbreviated as $\bar{V}_v/V_\infty = \alpha_0$. The ratio of the average inflow $\bar{V}_{in}$ to freestream velocity V_∞ is practically a linear function of T, and can be written as $\bar{V}_{in}/V_\infty = a - bT$. Solid, flat parachutes have about the same flow relationship.

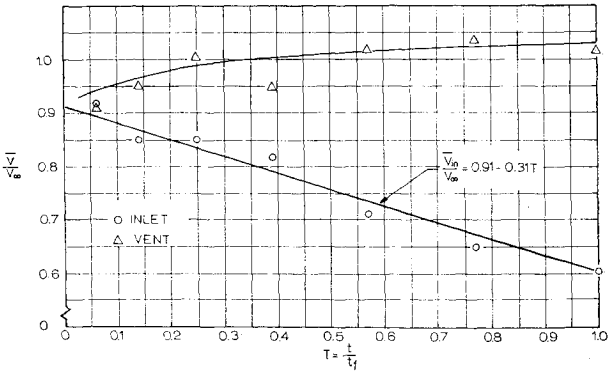

Fig. 4 Flow ratios through inlet and vent area of O'Hara shapes measured on rigid ribbon parachute model; λ_g = 35% under steady-state condition.[11]

The average velocity through the slots, V_g, is a function of the differential pressure and follows from $V_g = \eta(2\Delta p/\rho)^{1/2}$ with η an efficiency or flow coefficient,[7] and Δp the pressure differential between the inside and the outside of the parachute canopy. With the system velocity V_∞ it can also be shown that $\bar{V}_g/V_\infty = \eta(\bar{C}_p)^{1/2}$, where C_p is the pressure coefficient.

The flow coefficient η, also called the ribbon grid efficiency,[7] amounts to $\eta = \dot{m}/\dot{m}_i$, in which $\dot{m}$ and $\dot{m}_i$ are the actual and ideal mass fluxes through the slotted grids related to viscous and inviscid conditions. The actual mass flow through an area consisting of ribbon grids can be presented also by means of the coefficient of the effective porosity, $C = u/v$. In this expression, u is the average velocity over the porous or slotted area, and v an undisturbed freestream velocity.[7] With this definition and using V_∞ for v, the actual mass flow amounts to $\dot{m} = \rho S_0 u = \rho S_0 C V_\infty$. This can be related to the ideal mass flow and yields

$$\dot{m}/\dot{m}_i = \rho S_0 C V_\infty/\rho S_0 \lambda'_g V_\infty = C/\lambda'_g \qquad (5)$$

or, with the previous definition, $C = \lambda'_g\eta$. Using the so far defined terms, Eq. (4) assumes the form

$$\frac{dV}{dT} = \frac{t_f V_\infty D_0^2}{\pi}\left\{\frac{\pi^2}{4}\left(\frac{d}{D_0}\right)^2(a - bT) - \frac{\pi^2}{4}\left(\frac{d_v}{D_0}\right)^2\alpha_0 - \right.$$
$$\left. - \frac{\pi^2}{2}C\bar{C}_p^{1/2}\left[\left(\frac{D_p}{D_0}\right)^2 - \left(\frac{d_v}{4D_0}\right)^2\right]\right\} \qquad (6)$$

With the time functions d/D_0 and D_p/D_0, the integration of Eq. (6) yields the filling time t_f.

Applying O'Hara's[2] geometry, the inlet diameter d is related to the projected diameter D_p by

$$d/D_0 = (D_p/D_0)/(\tfrac{3}{2} - \pi/4\ D_p/D_0) \qquad (7)$$

For the ratio D_p/D_0 one can now use the size-time functions as discussed in Sec. II. For solid flat parachutes, it appears to be justified to use the relationship with the increasing potentials of T, whereas, for ribbon parachutes, the linear size-time history will be tried.

V. Solution for Solid Cloth Parachutes

With Eq. (7) and the size-time function known, Eq. (6) can be integrated. This may be cumbersome but not difficult. Furthermore, one may assume that the volume of the inflated canopy under steady-state conditions equals the volume of a hemisphere having the same diameter, namely, $D_{ps}/D_0 = 0.65$. The ratio of inflow to freestream velocity can be approximated[2] by $V_{in}/V_\infty = 1 - T$, which yields for solid, flat parachutes $a = b = 1$. After integration of Eq. (6), one notices repeatedly the term of $(d_v/D_0)^2$ which, in reality, is usually less than 0.005 and, compared with the other terms, can be neglected. This simplifies the result to such an extent

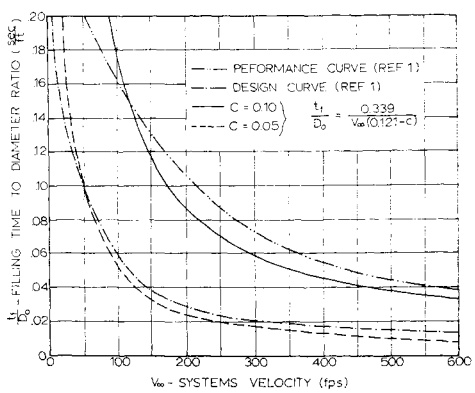

Fig. 5 Filling time of parachutes under infinite-mass condition.

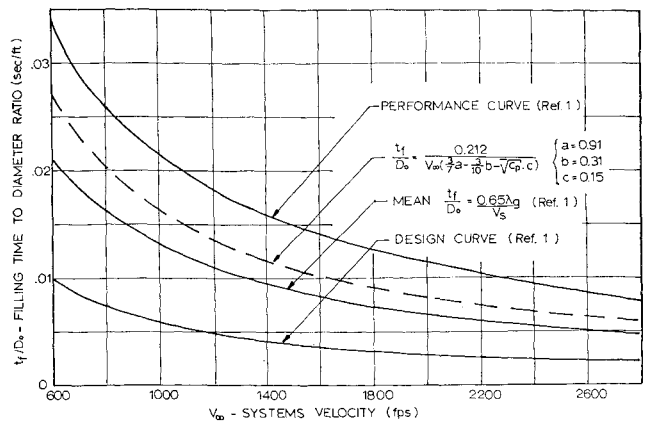

Fig. 6 Filling time of parachutes with inherent porosity under infinite-mass condition.

that Eq. (6) yields

$$V_\infty t_f/D_0 = 0.339/(0.121 - C) \qquad (8)$$

Equation (8) indicates that the filling time becomes infinite when the effective porosity amounts to $C_{crit} = 0.121$. An effective porosity of 0.12–0.13 represents a nominal porosity of approximately 340–365 ft³/ft²-min, and from experience one knows that with such a high porosity at sea-level density conventional parachutes usually fail to inflate.

Equation (8) can also be used to calculate a filling-time-diameter relationship vs velocity, which can be compared with experimentally established curves in Ref. 1, Fig. 5. The information in Ref. 1 has been actually obtained from experiments with ribbon parachutes with satisfactory porosity characteristics. However, no particular porosity values are specified. As can be seen, the curves derived in this analysis compare well with those recommended on the basis of experimental data.

VI. Solution for Ribbon and Ringslot Parachutes

The in- and out-flow relationship shown in Fig. 4 was obtained for a rigid ribbon parachute model with 33% geometric grid porosity, $\lambda'_g = 0.33$, and an over-all porosity of $\lambda_g = 0.35$. In accordance with these measurements, the inflow function amounts to $\bar{V}_{in} = V_\infty(0.91 - 0.31T)$, which yields $a = 0.91$ and $b = 0.31$. The same measurements also provided an average pressure coefficient during the filling period of approximately $(\bar{C}_p)^{1/2} = 1.12$.

The mass-balance equation (6) applies, of course, also to the inflation of ribbon or ringslot parachutes. Selecting in view of Fig. 3 a linear size-time function, one may utilize the geometric derivations of Ref. 1 and obtain $d/D_0 = 2/\pi T^{2/3}$ and $D_p/D_0 = 2/\pi T^{1/2}$.

With these functions, Eq. (6), for ribbon and ringslot parachutes, can be written as

$$dV/dT = V_\infty A\{aT^{4/3} - bT^{7/3} - B[\alpha_0 - C(\bar{C}_p)^{1/2}] -$$
$$-2C(\bar{C}_p)^{1/2}T\} \qquad (9)$$

For convenience, this equation contains the abbreviations $A = t_f D_0^2/\pi$ and $B = (\pi d_v/2D_0)^2$.

Using as upper boundary again the volume of a hemisphere, Eq. (9) can be evaluated for the filling time t_f. As before, the solution includes terms of $(d_v/D_0)^2$ which for ribbon parachutes at the most amounts to 0.0025. Neglecting these terms, introducing the values for a, b, and C_p, and arranging the solution accordingly, one obtains

$$V_\infty t_f/D_0 = 0.212/(0.296 - 1.12C) \qquad (10)$$

Equation (10) indicates a critical porosity of $C_{crit} = 0.264$, which is higher than we had before. This is probably the consequence of the flow conditions reflected in the terms of a and $b \neq 1$. As shown before, the effective porosity C is related to the geometric porosity λ_g through the flow coefficient η. Nylon grids have flow coefficients up to approximately $\eta = 0.85$,[7] and in view of Eq. (10), the critical geometric porosity value is approximately $\lambda'_{gcrit} = 31\%$. This agrees well with established experimental data, since it is known that ribbon parachutes with geometric porosities of 30% and higher have, in general, uncertain inflation characteristics.

The validity of Eq. (10) can also be checked by comparing a calculated curve with those recommended in Ref. 1. For this purpose, an effective porosity of $C = 0.15$ has been selected, which is suitable for ribbon as well as ringslot parachutes. Assuming an efficiency factor of $\eta = 0.85$, the effective porosity, $C = 0.15$, represents a geometric porosity $\lambda'_g = 17.6\%$. This is an accepted porosity value for conventional parachutes. The calculated and the experimental curves are shown in Fig. 6, and one notices that the calculated curve follows closely the mean experimental curve recommended in Ref. 1.

In view of the agreement between the calculated and experimentally obtained opening times for ribbon and ringslot parachutes, it appears that the assumption of a linear size-time function as first approximation is satisfactory for calculations of performance data.

A better approximation, somewhat similar to the one used for solid, flat parachutes, may be introduced when the size-time relationship of parachutes with inherent porosity under finite-mass condition is more reliably established.

VII. Summary

The infinite-mass condition is defined as a ratio between the masses of the suspended weight and the included air. Using this definition, the continuity equation, combined with experimentally established size-time functions and a certain parachute geometry during inflation, has provided solutions the results of which compare well with experimentally established parachute filling times.

References

[1] "Performance of and Design Criteria for Deployable Aero-Dynamic Decelerators," *United States Air Force Parachute Handbook*, TR ASD-TR-61-579, Dec. 1963, Aeronautical Systems Div., Air Force Systems Command.

[2] O'Hara, F., "Notes on the Opening Behavior and the Opening Forces of Parachutes," *Royal Aeronautical Society Journal*, Nov. 1949.

[3] Heinrich, H. G. and Noreen, R. A., "Analysis of Parachute Dynamics with Supporting Wind Tunnel Experiments," AIAA Paper 68-924,El Centro, Calif., 1968.

[4] Pflanz, E., "Zur Bestimmung der Verzoegerungskraefte bei Entfaltung von Lastenfallschirmen," ("Calculation of the Deceleration Forces of Parachutes") ZWB/FB/1706/2 (ATI 26111), Sept. 1943, Forschungsanstalt Graf Zeppelin, Ruit ueber Esslingen.

[5] Berndt, R. J., "Experimental Determination of Parameters for the Calculation of Parachute Filling Times," Jahrbuch des Wissenschaftlichen Gesellschaft fuer Luft- und Raumfahrt E.V. (WGLR), 1964, pp. 299-316.

[6] Berndt, R. J. and DeWeese, J. H., "Filling Time Prediction Approach for Solid Cloth Type Parachute Canopies," *AIAA Aerodynamic Deceleration Systems Conference*, AIAA, New York, 1966.

[7] Heinrich, H. G., "The Effective Porosity of Ribbon Grids," *Zeitschrift fuer Flugwissenschaften* 14, Heft 11/12, Verlag Friedr. Vieweg & Sohn GmbH, Braunschweig, 1966.

[8] Heinrich, H. G., "The Effective Porosity of Parachute Cloth," *Zeitschrift fuer Flugwissenschaften* 11, Heft 10, Verlag Friedr. Vieweg & Sohn, Braunschweig, 1963.

[9] Smetana, F. O., "On the Determination of Parachute Cloth Permeability," *Zeitschrift fuer Flugwissenschaften* 14, Heft 10, Verlag Friedr. Vieweg & Sohn GmbH, Braunschweig, 1966.

[10] Hellenbeck, G. A., "The Magnitude and Duration of Parachute Opening Shocks at Various Altitudes and Air Speeds," Memo Rept. ENG 49-696-66, 1944, U.S. Air Force.

[11] Buchanan, K. B., "Experimental Determination of the Subsonic Mass Flow Through Several Ribbon Type Parachute Canopies During Inflation and at Steady State Conditions," AFFDL-TR-67-165, Air Force Flight Dynamics Lab., Wright-Patterson Air Force Base, Ohio, April 1968.